



Finite Element Analysis and Fabrication of a 3 MHz Megasonic System for Semiconductor Cleaning

Hyunse Kim^{a,b*}, Euisu Lim^a, Yanglae Lee^a^aInnovative Energy Machinery Research Division, Korea Institute of Machinery and Materials^bDepartment of Mechanical Engineering, University of Science & Technology

ARTICLE INFO

Article history:

Received	6	May	2022
Revised	31	May	2022
Accepted	2	June	2022

Keywords:

Megasonic
Cleaning
Finite element method(FEM)
Waveguide
Piezoelectric actuator

ABSTRACT

Megasonic cleaning has been used to clean contaminants from wafer surfaces in semiconductor production. This research developed a 3 MHz megasonic waveguide for cleaning processes in semiconductor industries. Firstly, a 1 MHz type was fabricated in aluminum (Al) and quartz, consisting of a lead zirconate titanate (PZT) actuator and a waveguide. A 3 MHz quartz waveguide was also fabricated based on the fabricated results, and its performance was tested. In the design process, finite element analysis was performed. As a result, the predicted value was 2.997 MHz, which agreed with the measured value of 2.995 MHz with a 0.1% error. Lastly, a particle removal efficiency (PRE) test was performed, and the results showed that 93.1% PRE was achieved at 8W power. Considering the acoustic pressure and the cleaning test results, the 3 MHz megasonic may help the removal of contaminants from wafer surfaces effectively.

1. Introduction

In manufacturing semiconductors, several processes are involved, which include film deposition, photoresist (PR) coating, photolithography, etching, and cleaning. After each step, cleaning processes are required. As pattern sizes are shrinking, cleaning criteria have become very strict. Generally, either standard cleaning-1 (SC-1) or SC-2 is used. SC-1 solution is a mixture of H₂O₂ and NH₄OH diluted by deionized water with ratios of H₂O₂:NH₄OH:deionized water of 1:1:5. The other solution is SC-2 solution, which involves a hydrochloric acid / hydrogen peroxide mixture (=HPM). A drawback of these chemical cleaning is the limit of particle size that can be removed due to van der Waals force, as follows:

$$F_{vdw} = \frac{AR}{6z^2} \quad (1)$$

where, F_{vdw} is the van der Waals force, A is the Hamaker constant, R is the radius of a particle, and z is the distance between the particle and substrate^[1]. The gravitational force at macro scale, which is proportional to the mass ($\propto R^3$), is almost negligible. Thus, F_{vdw} prevents a nano-size particle from being detached from a wafer surface. Hence, physical forces, such as ultrasonic or megasonic agitation, have been added.

Ultrasonic wave means a sound in an inaudible frequency range over 20 kHz. It has been applied in many industrial areas. First, it can help metal machining, such as drilling, surface reformation, milling, and so on. Recently, Liu et al. reported an ultrasonic peening drilling (UPD)^[2], which could achieve strengthening and precision-machining in

* Corresponding author. Tel.: +82-2-868-7967

E-mail address: hkim@kimm.re.kr (Hyunse Kim).

finishing a hole drilling process. We also reported a 20 kHz ultrasonic system for nano-surface reformation process^[3]. Additionally, we developed an ultrasonic milling system by finite element analysis^[4]. Regarding burnishing, Su et al. reported the strengthening of titanium alloy by ultrasonic roller burnishing^[5]. For polishing application, Yang et al. performed research into an ultrasonic vibration assisted electrochemical mechanical polishing for 4H-SiC wafers^[6]. Li et al. published a grinding force model in two-dimensional ultrasonic-assisted grinding^[7]. Lastly, Ni et al. reported research into the interfacial bonding mechanism and fracture behavior in the ultrasonic spot welding of copper sheets^[8].

Megasonics were introduced decades ago, and are still under development for application to semiconductor industries. These are systems that adapt ultrasonics of more than 1 MHz frequency. They can help remove nano-sized particles using physical agitation by the vibration of the megasonic waves. We also report some research regarding a 1 MHz L-type and a Horn-type megasonic waveguide for nanoparticle cleaning^[9,10]. Keswani et al. introduced a method based on electrochemical impedance spectroscopy (EIS) measurements for the detection of transient cavity collapses in megasonic^[11]. Hauptmann et al. reported the effect of gasification on the performance of a megasonic cleaning system^[12].

Thus, due to pattern damage probabilities, the technology should be carefully used. Although these issues remain, attempts to lower the problems have been made by optimizing process conditions, such as chemicals. Hence it is beneficial to develop effective megasonic waveguides. Generally, as the frequency of a megasonic system increases, the output power decreases reversely. To reduce patten damages, we decided to raise operating frequency up to 3 MHz.

In this article, we describe the design process and experiments of a 1 MHz and a 3 MHz megasonic cleaning system. First, we developed the 1 MHz megasonic system, because the 3 MHz type was thought to be too sensitive. Then, based on the result of the 1 MHz type, we designed and fabricated a 3 MHz megasonic. In the design process, finite element method (FEM) was applied to predict the impedance characteristics. It is necessary to design the lead zirconate titanate (PZT) actuator and the waveguide, which can generate and transfer the wave energy. A 1 MHz prototype was fabricated, and the performance was tested. The 3 MHz type was then designed, and fabricated. At this time, acoustic pressures were measured, and particle removal efficiency (PRE) was also measured through cleaning

wafer tests.

2. Design of megasonic waveguides

2.1 1 MHz megasonic fabrication and tests

First, the 1 MHz type was developed, which can show relatively strong output power. The displacement at the end of the waveguide is inversely proportional to the frequency according to the following equation:

$$v = f \cdot \lambda \quad (2)$$

where, v is the velocity of the wave, f the frequency, and λ the wavelength. This equation means that when the v is the same, higher f induces lower λ . If λ is lower, then the wave emitted from the end of the waveguide is also shorter. Thus, lower frequency of 1 MHz type was thought to be easier to develop. The 1 MHz waveguide cleaning system consists of a piezoelectric actuator, a waveguide, and an electric generator, which supplies power to the piezoelectric actuator.

Due to the easiness of machining, the aluminum (Al) waveguide was fabricated in advance. In contrast, the machining process of the quartz material is generally complicated. First the raw material of the cylinder shape is cut. Then, the desired shape is machined with conventional machining process. Next, the surface is ground. The 1 MHz waveguide was symmetrical and of cylindrical shape, thus further process was not required. Fig. 1(a) shows the fabricated 1 MHz aluminum (Al) waveguide, and Fig. 1(b) the quartz type.

For actuation, an electric generator is required, as shown in Fig. 2. The generator emits sine wave electricity to the piezoelectric actuator. Then the displacement is generated, which is caused by the resonance motion of the waveguide. Thus, the acoustic power from the end of the waveguide, can be used to remove the contaminated particles from wafer surfaces. The electric generator is composed of control panel

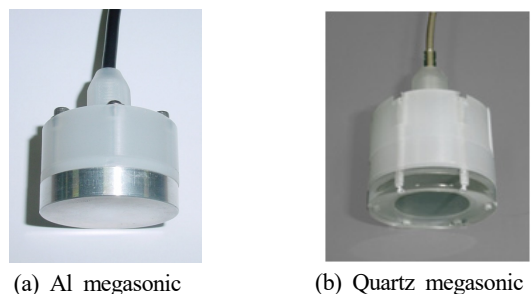


Fig. 1 1 MHz megasonic waveguide



Fig. 2 Electric generator

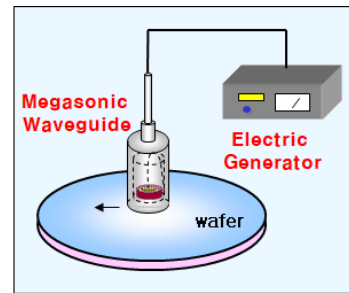
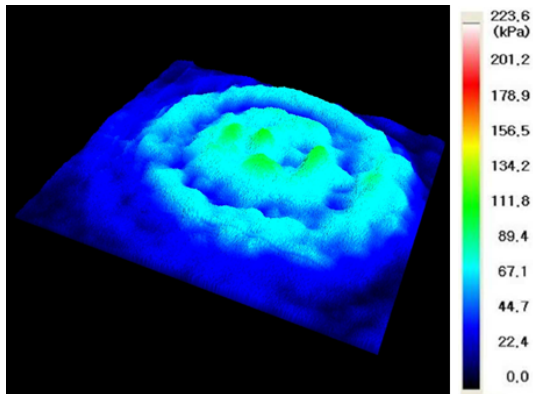
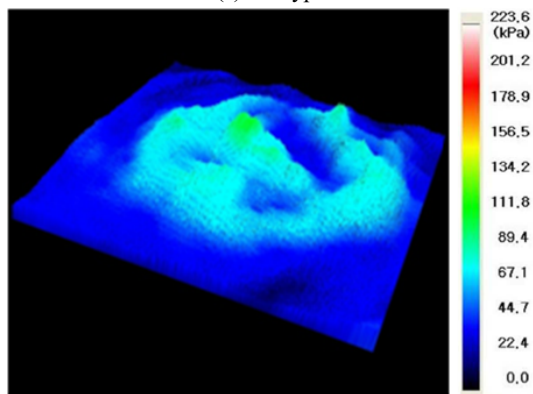


Fig. 4 Structure and working principle of the 3 MHz quartz megasonic system



(a) Al type



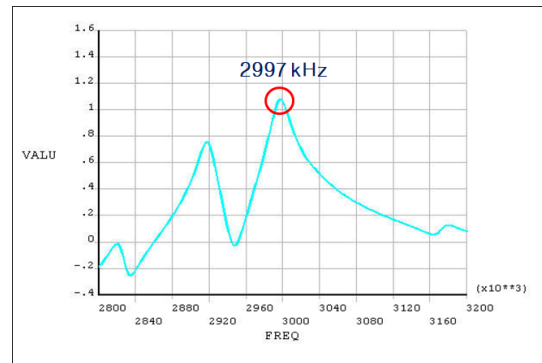
(b) Quartz type

Fig. 3 Acoustic pressure distributions

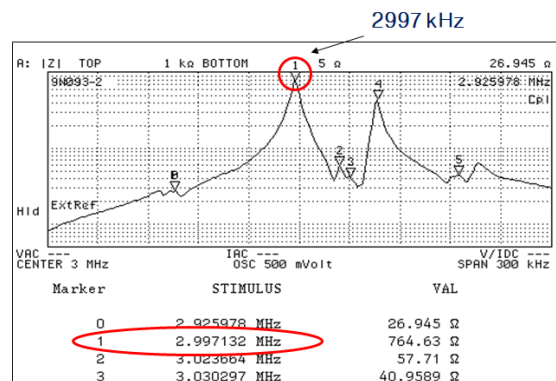
267%, and standard deviation/average ratio was 45%. These values explain the relatively mild acoustic pressure distributions.

2.2 A 3 MHz megasonic fabrication

Using these results, the 3 MHz type was fabricated, which has lower output power, while showing more uniform acoustic pressures. As mentioned in the previous chapter, the displacement will be 1/3, compared to the 1 MHz frequency type. Fig. 4 shows the structure and working principle of the 3 MHz type. The system is composed of the waveguide, and the electric generator. The waveguide is placed over a wafer,



(a) FEM result

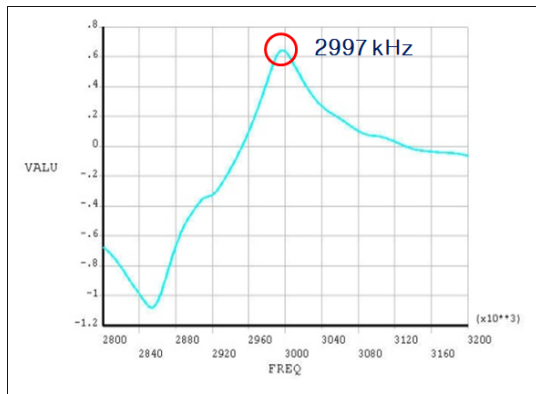


(b) Experimental result

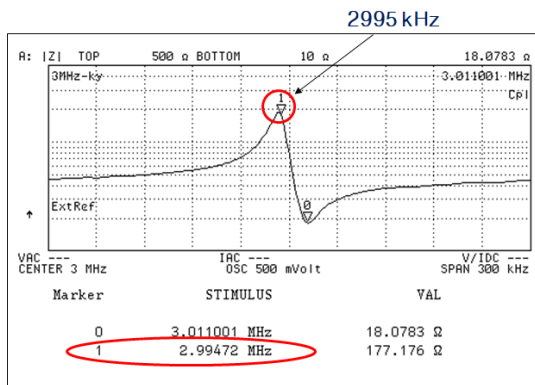
Fig. 5 3 MHz PZT impedance graphs

and electric circuits inside. From the control panel, the power can be switched on/off, and the intensity of the power can be controlled using the buttons.

After manufacturing the PZT and the quartz waveguide, the acoustic pressures were measured. Fig. 3(a) shows the results for the Al type, and Fig. 3(b) the quartz type. Relatively well-distributed pressure could be observed in both types. For analysis, we calculated the average, maximum, and standard deviation. As a result, the maximum/average was 272%, and the standard deviation/average was 59% for the Al type. In addition, the maximum/average ratio for the quartz type was



(a) FEM result



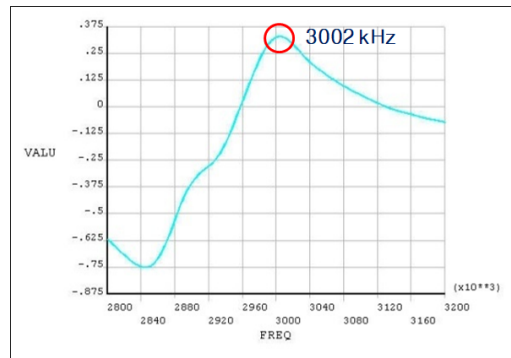
(b) Experimental result

Fig. 6 3 MHz waveguide impedance graphs

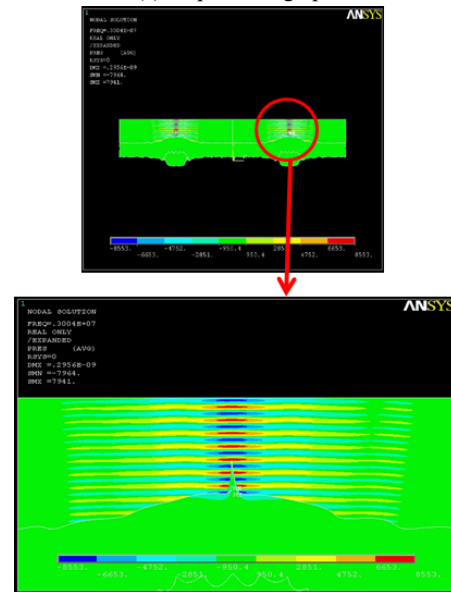
and it moves slowly from the center to the outside. At the same time, the wafer is rotated slowly. Thus, the whole surface can be scanned with the megasonic wave, so that the contaminants can be detached and washed away by the supplied deionized (DI) water.

In the development process, we firstly performed FEM analysis for the PZT. Fig. 5(a) shows the 3 MHz PZT impedance graph of FEM, while Fig. 5(b) explains the experimentally measured impedance graph. As seen in the figures, the predicted value was 2.997 MHz, which coincided with the measured value. At this time, using the same analytical procedures, the waveguide with the 3 MHz actuator was designed. As a result, Fig. 6(a) shows the 3 MHz waveguide impedance graph of FEM, and Fig. 6(b) is the experimentally measured graph. The predicted value was 2.997 MHz, which agreed well with the measured value of 2.995 MHz with 0.1% error.

Then, the 3 MHz PZT impedance graph of the FEM with water was calculated. As shown in Fig. 7(a), the predicted impedance value was 3,002 kHz. This value was increased by 2 kHz compared to the impedance, when there was no water. In addition, the acoustic pressures in the water were simulated, and the distributions are shown in Fig. 7(b). Evenly



(a) Impedance graph



(b) Acoustic pressure distributions

Fig. 7 Acoustic analysis of the 3 MHz waveguide with water by FEM



Fig. 8 The 3 MHz megasonic waveguide

distributed pressures could be found, which can be used in understanding the water behavior.

Using these FEM results, a quartz material waveguide was fabricated, as shown in Fig. 8. The bottom of the waveguide is shown with transparent image, so that the ring-type white PZT actuator can be seen.

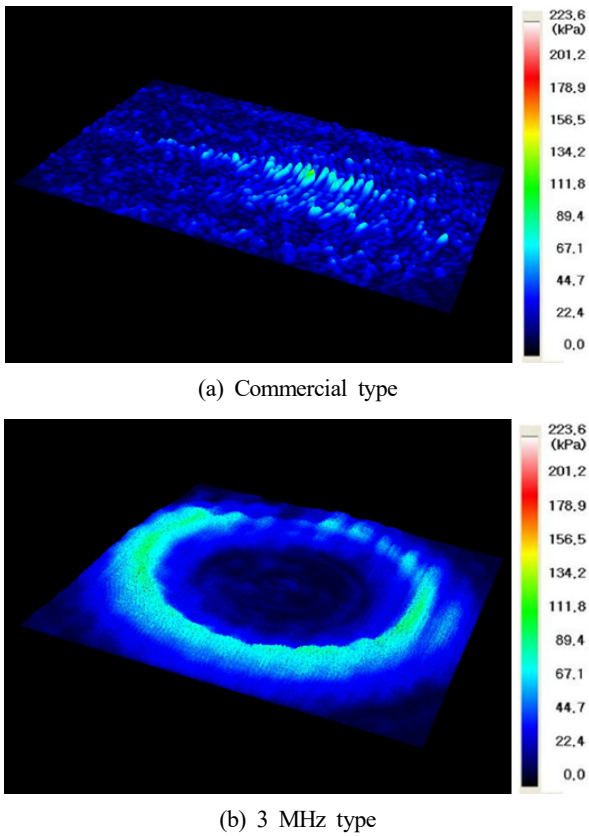


Fig. 9 Acoustic pressure distributions

3. Experiment

For the assessment of the developed product, the acoustic pressures of the developed one and a commercial one, were measured and compared. The measured result of the developed one is shown in Fig. 9(a), and the commercial type in Fig. 9(b). The developed one showed relatively regular distributions having a ring-shape, which indicate the PZT shape. For the analysis of the system performances, acoustic pressures were measured with different input powers.

Fig. 10(a) shows the acoustic pressure measurement results of maximum values, and Fig. 10(b) the standard deviations. Compared to the conventional A-type, the maximum value was decreased by 36–45%, and the standard deviation was diminished by 10–12%. Higher average implies higher output level, which means more power for cleaning. In addition, lower maximum values and standard deviations indicate less possibility of pattern damage. Thus, the developed product shows better performance.

Then, cleaning test using silica particles were performed. Silica particles which sizes are 80 nm were deposited on a bare wafer, and the particle number was counted. Next, the

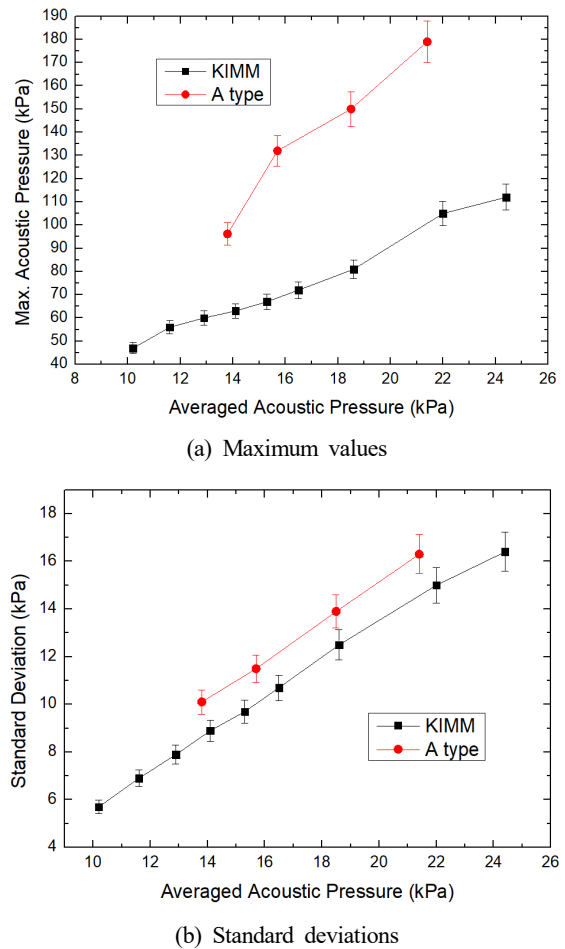


Fig. 10 Acoustic pressures measurement results

particles were cleaned with our developed system and the remained particle number was counted. Figs. 11(a) and (b) show the cleaning test results of before (9,532) and after (658) at 8 W power. Particle removal efficiency (PRE) of over 93.1% was achieved at this condition. We repeated the cleaning tests with different powers. As can be seen in Fig. 12, over 90% PRE could be obtained over 5 W.

4. Conclusion

In this work, a 3 MHz megasonic cleaning system was designed, and fabricated. First, the 1 MHz megasonic was developed, and the acoustic pressures were measured. Using these results, the 3 MHz type was designed and fabricated. In the design process, finite element analysis was performed to predict the impedance characteristics of the actuator and the waveguide. As a result, following conclusions were obtained:

- (1) The maximum/average ratio of the 1 MHz megasonic acoustic pressures, was 272%, and the standard deviation/

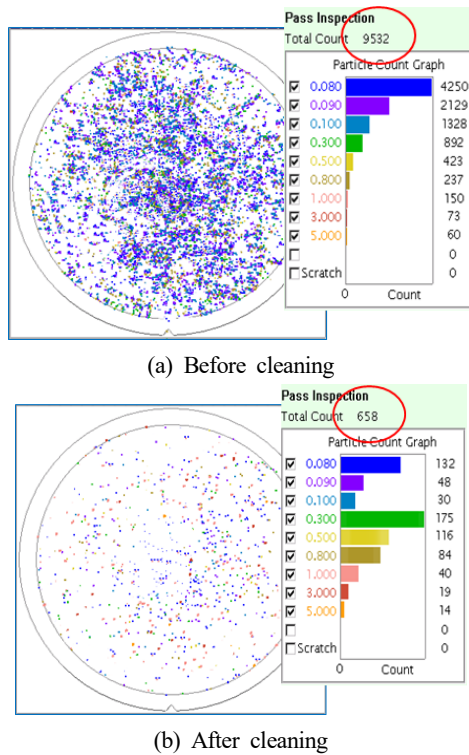


Fig. 11 Cleaning test results

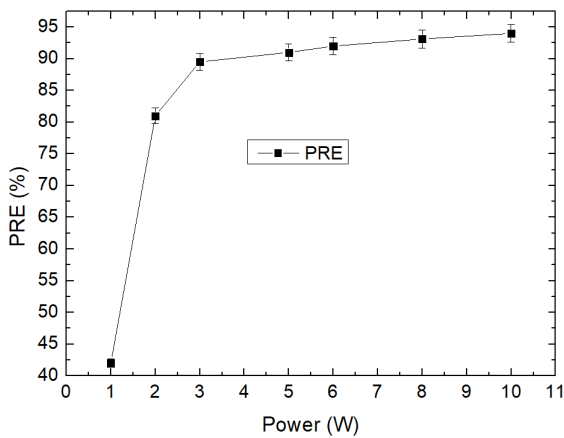


Fig. 12 PRE graph

average ratio was 59% for the Al type.

(2) In addition, the maximum/average ratio for the quartz type was 267%, and the standard deviation/average ratio was 45%. These values meant relatively mild acoustic pressure distributions.

(3) The 3 MHz waveguide impedance graph of FEM was predicted as 2.997 MHz, which agreed well with the measured value of 2.995 MHz with 0.1% error.

(4) Regarding the acoustic pressure, compared to the conventional A-type, the maximum value was decreased by 36–45%, and the standard deviation was diminished by 10–12%.

(5) Finally, cleaning tests were performed, and over 90% PRE could be obtained over 5 W. Considering the acoustic pressure and the cleaning test results, the 3 MHz megasonic system might help with the effective removal of contaminants from wafer surfaces.

Acknowledgement

This research was supported by the Korea Evaluation Institute of Industrial Technology (KEIT), under the Korea government Ministry of Knowledge Economy and by a research project (NK237C) of the Korea Institute of Machinery and Materials (KIMM).

References

- [1] Kanegsberg, B., Kanegsberg, E., 2000, Handbook for Critical Cleaning, CRC Press, Boca Raton, U.S.A..
- [2] Liu, Y., Geng, D., Shao, Z., Zhou, Z., Jiang, X., Zhang, D., 2021, A Study on Strengthening and Machining Integrated Ultrasonic Peening Drilling of Ti-6Al-4V, Materials & Design, 212 110238, <https://doi.org/10.1016/j.matdes.2021.110238>.
- [3] Kim, H., Lim, E., Lee, Y., Park, J.-K., 2019, Fabrication and Performance Tests of an Ultrasonic Cleaning System for Solar-cell Wafers, J. Korean Soc. Manuf. Technol. Eng., 28:4 210-217, <https://doi.org/10.7735/ksmte.2019.28.4.210>.
- [4] Kim, H., Lim, E., Park, J.-K., 2017, Development of a 20 kHz Ultrasonic System for Nano-surface Reformation Process, J. Korean Soc. Manuf. Technol. Eng., 26:4 365-370, <https://doi.org/10.7735/ksmte.2017.26.4.365>.
- [5] Su, H., Shen, X., Xu, C., He, J., Wang, B., Su, G., 2020, Surface Characteristics and Corrosion Behavior of TC11 Titanium Alloy Strengthened by Ultrasonic Roller Burnishing at Room and Medium Temperature, J. Mater. Res. Technol., 9:4 8172-8185, <https://doi.org/10.1016/j.jmrt.2020.05.059>.
- [6] Yang, X., Yang, X., Gu, H., Kawai, K., Arima, K., Yamamura, K., 2022, Efficient and Slurryless Ultrasonic Vibration Assisted Electrochemical Mechanical Polishing for 4H-SiC Wafers, Ceram. Int., 48:6 7570-7583, <https://doi.org/10.1016/j.ceramint.2021.11.301>.
- [7] Li, H., Chen, T., Duan, Z., Zhang, Y., Li, H., 2022, A Grinding Force Model in Two-dimensional Ultrasonic-assisted Grinding of Silicon Carbide, J. Mater. Process Technol., 304 117568,

<https://doi.org/10.1016/j.jmatprotec.2022.117568>.

- [8] Ni, Z. L., Liu, Y., Wang, Y. H., He, B. Y., 2022, Interfacial Bonding Mechanism and Fracture Behavior in Ultrasonic Spot Welding of Copper Sheets, *Materials Science and Engineering: A*, 833 142536, <https://doi.org/10.1016/j.msea.2021.142536>.
- [9] Kim, H., Lee, Y., Lim, E., 2009, Design and Fabrication of an L-type Waveguide Megasonic System for Cleaning of Nano-scale Patterns, *Curr. Appl. Phys.*, 9:2 e189-e192, <https://doi.org/10.1016/j.cap.2008.12.058>.
- [10] Kim, H., Lee, Y., Lim, E., 2013, Design and Fabrication of a Horn-type Megasonic Waveguide for Nanoparticle Cleaning, *IEEE Trans. on Semiconductor Manufacturing*, 26:2 221-225, <https://doi.org/10.1109/TSM.2013.2238563>.
- [11] Keswani, M., Raghavan, S., Deymier, P., 2013, A Novel Way of Detecting Transient Cavitation Near a Solid Surface during Megasonic Cleaning using Electrochemical Impedance Spectroscopy, *Microelectron. Eng.*, 108 11-15, <https://doi.org/10.1016/j.mee.2013.02.097>.
- [12] Hauptmann, M., Brems, S., Camerotto, E., Zijlstra, A., Doumen, G., Bearda, T., Mertens, P.W., Lauriks, W., 2010, Influence of Gasification on the Performance of a 1 MHz Nozzle System in Megasonic Cleaning, *Microelectron. Eng.*, 87:5-8 1512-1515, <https://doi.org/10.1016/j.mee.2009.11.06>.



Hyunse Kim

Principal researcher in the Innovative Energy Machinery Research Division, Korea Institute of Machinery and Materials, and a Professor in University of Science & Technology. His research interest is ultrasonic cleaning, megasonic cleaning and ultrasonic machining.
E-mail: hkim@kimm.re.kr



Euisu Lim

Principal technician in the Innovative Energy Machinery Research Division, Korea Institute of Machinery and Materials. His research interest is ultrasonic and megasonic cleaning.
E-mail: eslim@kimm.re.kr



Yanglae Lee

Principal researcher in the Innovative Energy Machinery Research Division, Korea Institute of Machinery and Materials. His research interest is ultrasonic and megasonic cleaning.
E-mail: yllee@kimm.re.kr